CNRS
*Centre National de la Recherche Scientifique*

INFN
*Istituto Nazionale di Fisica Nucleare*

# Analysis of spectral lines in run C7

I. Fiori, F. Paoletti, E. Cuoco
*EGO*
N. Christensen
*Carleton College Northfield Minnesota*
G. Vajente
*SNS and INFN Pisa*

Reference: **VIR-NOT-EGO-1390-339 or VIR-031B-07**
Issue: 2
Date : 4/10/2007

**Abstract**

We describe the work of detection and identification of frequency lines in the Virgo dark fringe data from run C7. Among the topics of this note we highlight: (i) the new list of line candidates from the pulsars search analysis; (ii) investigation of the 10 Hz harmonics; (iii) violin modes; (iv) noise from the NE and WE buildings air conditioners; (v) sidebands in calibration lines; (vi) aliasing noise in the 4kHz reconstructed data.

EGO, European Gravitational Observatory
Via E. Amaldi - 56021 Santo Stefano a Macerata-Cascina-Pisa-Italy
Telephone +39.050.752521 - Fax +39.050.752550

# 1 Introduction

In this note we describe our work on the detection and investigation of the origin of the frequency lines in the Virgo dark fringe data from run C7. A number of data analysis techniques and experimental methods (in the laboratory) we used to identify and characterize these noise lines. We initially generated a first selection of frequency lines using the search algorithm described in reference [1] (Section 2). Line candidates also come as the by-product of the analysis pipeline of the periodic signal searches (PSS) performed by the Virgo pulsar search group. We discuss this new line catalog in Section 2 and compare the results with the outcome of the first search method. We also used a newly implemented catalogue of environmental coherences [3] and the multi-coherence tool [9] to investigate for the origin of environmental lines. We searched for a match between our line candidates and large coherence values with environmental channels (Section 3). Then we hunted for the sources of these lines by surveying the experimental halls with portable measurement equipment (spectrum analyzer, accelerometer, Hall probe, microphone). We identified some lines as originating from the WE and NE air conditioning; we also found the source of the 10 Hz noise line (Section 6). Other lines that were identified include: mirror modes and violin modes of mirror wires (Section 7, includes a measurement of ring-down decay time), sidebands of calibration lines (Section 4), and lines due to the residual aliasing in the 4kHz down-sampled data (Section 8).

# 2 Lines from the search algorithm

We produced one preliminary list of persistent frequency peaks ("lines") by applying the line search algorithm described in reference [1] to the dark fringe photodiode signal (channel *Pr_B1_ACp*). We processed the complete dataset of C7 science mode data (about 100 hours) by requiring the quality flag *Qc_Moni_ScienceMode* to be one. We used the algorithm parameters: SNR threshold=5, FFT resolution $\sigma_f = 1/13.1072s \simeq 0.07Hz$, 18 (non overlapping) averages. The spectral background was estimated using a tiling of the frequency axis of dyadic type, with parameters Nb=8, Nn=64, Nq=32[1].

The output of the algorithm over the entire C7 science mode dataset (approximately 110 hours) consists of 61516 frequency peaks. From this map of time-frequency data points we extracted a list of 70 *lines* by doing the following:

1. Remove 50 Hz harmonics (the $n^{th}$ harmonic is identified as the group of points within the frequency window of width $n \times \sigma_f$ around the frequency value $n \times 50$);
2. Select "persistent" frequencies, existing for at least 3% of total time;
3. Merge frequencies in nearby consecutive frequency bins, then assign to the candidate line the average frequency value and a *line width* equal to $\sigma_f$ times the number of merged lines.

These lines are listed in Table A1 (Appendix). Some frequencies are known from previous investigations, such as those from the vacuum pumps [15] and mirror thermal modes [13]. In the following Sections, 3 to 8, we describe the work of identifying the origin of the still unknown lines. In Section 3 we also comment on homogeneous groups of detected lines.

# 3 Lines from the pulsars search

Having identified most lines in Table A1, we looked for a more comprehensive list of lines. A list of persistent and high resolution frequency peaks comes almost for free from the search for periodic GW signals from pulsars [2]. The pulsar

[1] The algorith works in the frequency domain and proceedes in three steps: 1) computes the amplitude spectum of the dark fringe photodiode channel ($Pr\_B1\_ACq$) and subdivides the frequency axis in $N_b$ intervals of (minimum) lenght $N_n$ (data points); 2) in each interval makes a linear fit of the data points, excluding the $N_q$ points with the larges amplitude: this fit estimates the background spectral noise; 3) finally, within each interval selects data points which exceeds in amplitude the background by more than SNR times: these are the candidate lines. Two types of tiling of the frequency axis are defined: if $N_n N_b < N/2$ (*N* = number of FFT points) the tiling is dyadic for which the size of the interval increases with frequency (he smallest interval being of size $N_n$); if $N_n N_b = N/2$ the freqeuncy axis is tiled uniformly (all intervals have size $N_n$).

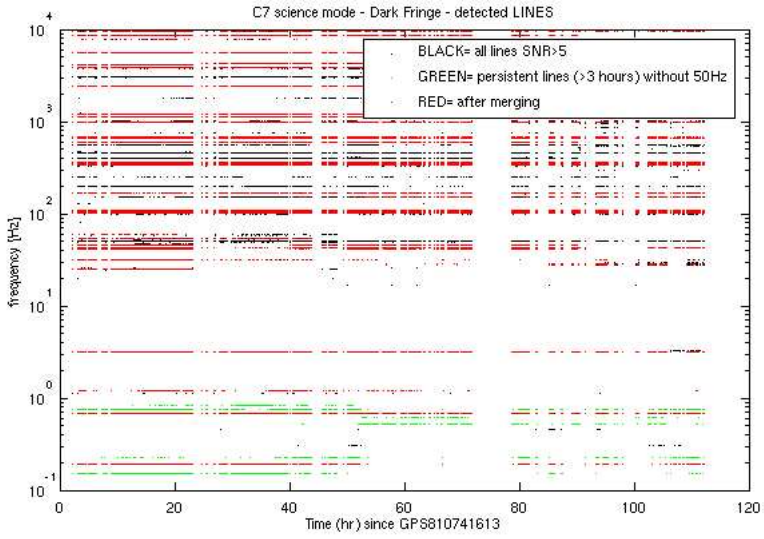


Figure 1: Time-frequency map of frequency peaks detected by the search algorithm [1] applied to C7 dark fringe science mode data segments (black). There were 61516 frequency peaks above the SNR threshold, corresponding to 772 different frequencies. This reduces to 155 persistent ones (see text), and finally reduces to 71 lines candidates (plus 18 50Hz harmonics) after merging nearby frequencies.

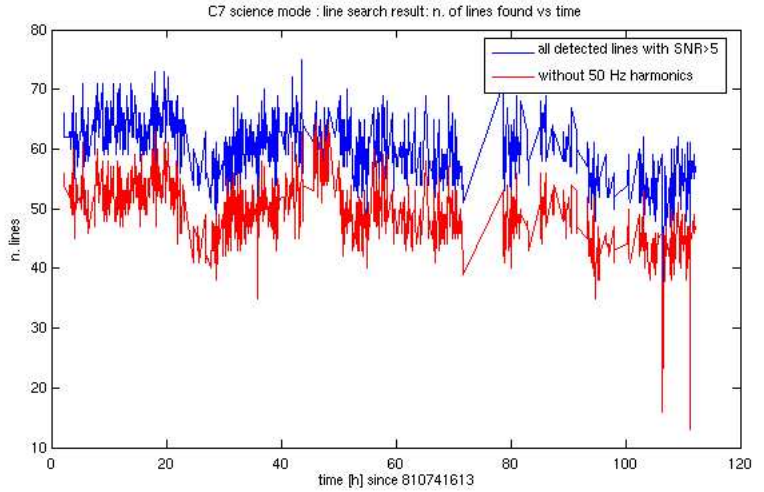


Figure 2: Number of frequency peaks detected by the line search algorithm in C7 dark fringe as function of time. In red: after removing all 50Hz multiples.

| Serial n. | Frequency (Hz) | N. recurrencies |
|---|---|---|
| 1 | 353.00 | 944 |
| 2 | 103.00 | 776 |
| 3 | 357.00 | 698 |
| 4 | 107.00 | 669 |
| 5 | 667.78 | 625 |
| 6 | 336.96 | 577 |
| 7 | 334.12 | 570 |
| 8 | 333.89 | 566 |
| 9 | 333.99 | 563 |
| 10 | 670.33 | 561 |
| 11 | 667.97 | 561 |
| 12 | 667.75 | 558 |
| 13 | 1001.69 | 548 |
| 14 | 334.55 | 547 |
| 15 | 669.21 | 545 |
| 16 | 334.46 | 544 |
| 17 | 667.85 | 538 |
| 18 | 337.14 | 538 |
| 19 | 333.31 | 535 |

Table 1: The twenty most persistent frequency peaks from the PSS list. The third column lists the number of FFTs in which the peak appears, as explained above. The complete list can be found at $http://wwwcascina.virgo.infn.it/DataAnalysis/Noise/doc/-C7/Lines/sergio\_frasca\_peaks.dat$).

search group set up an analysis procedure to search for periodic signals (PSS) in the Virgo strain sensitivity channel. As described in reference [2], the PSS analysis pipeline first performs a data cleaning, identifying and removing transient time domain disturbances. Then it produces collections of FFTs of various lengths over the entire science mode dataset. The subsequent step consists in the adaptive search for frequency peaks in these spectra. To do this they compute an auto regressive average spectrum which gives a good estimate of the spectral background noise; they then take the ratio of the FFT to the average spectrum and select the data that exceeds a given threshold SNR.

The results that the PSS group provided us with contains the list of frequency peaks and their significance, i.e. the number of FFTs containing that peak (note that a peak which exists only for a fraction of the total time has a low significance number). The first 20 peaks, ordered by decreasing significance, are listed in Table 1. These data were produced using the C7 strain reconstructed channel down-sampled to 4kHz (*hrec_4kHz*) and an FFT resolution of $T_{window}$=1048.6s (4194314 data points at 20kHz) over the frequency range 0 to 2000Hz. This was sufficient for our purposes.

We stress that PSS also produces datasets of frequency peaks from higher resolution FFTs. Presently three datasets are generated: $T_{window}$=4000s and $f_{max}$=500Hz, $T_{window}$=8000s and $f_{max}$=125Hz, $T_{window}$=16000s and $f_{max}$=31.25Hz. These could be used to probe lines of decreasing intensity. The PSS peaks list includes all of the lines given in Table A1, plus many more that emerged from background noise because of the higher resolution used. In particular, Figure 3 has a plot of the values of PSS list between 0 and 3 Hz; these are likely resonant modes of the mirror suspensions. This is discussed in Section 4 below.

In Figure 4 we plot the values of PSS list between 5 and 50 Hz. Most of these frequency peaks are generated by electro-mechanical devices. In Section 5 we describe the work on the identification of these lines. In summary, the lines we identified in the PSS list belong to seven categories, which we describe in more detail in the following sections:

1. oscillation modes of the super attenuators (Section 4);
2. sidebands of calibration lines (Section 4);
3. environmental lines (Sections 5 and 6);

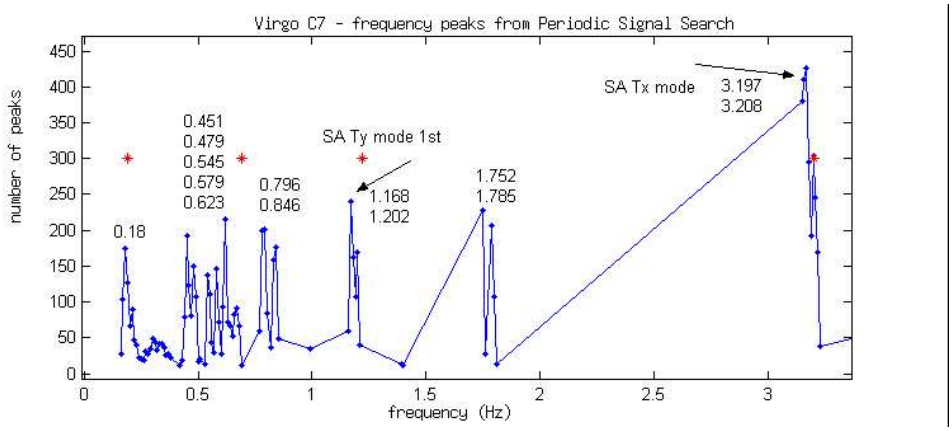


Figure 3: Very low frequency peaks (0 to 3Hz) from the periodic signals search analysis (on the vertical axis is the number of recurrences in the entire C7 *hrec_4kHz* channel)

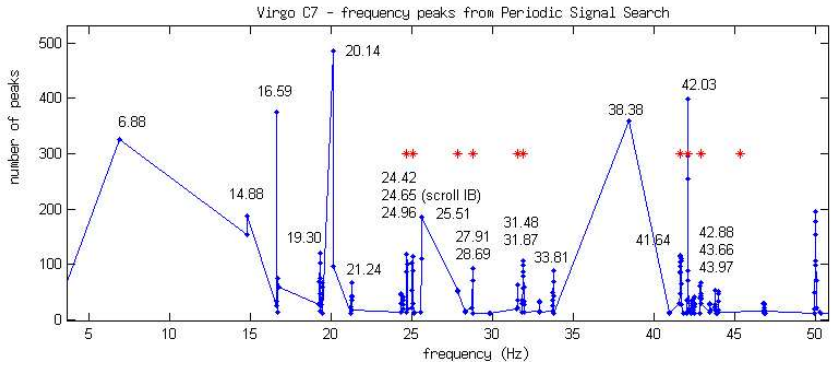


Figure 4: Low frequency peaks (5 to 50 Hz) from the periodic signals search analysis (on the vertical axis is the number of recurrences in the entire C7 *hrec_4kHz* channel).

4. 10 Hz and harmonics (Sections 5 and 13, see also reference [4]);
5. thermally excited modes of the mirror mass (Section 7);
6. violin modes of mirrors' wires (Section 7);
7. aliased lines (Section 8).

# 4 SA modes and sidebands of calibration lines

Very low frequency peaks (up to 3.2 Hz, see Figure 3) are oscillations of the mirrors at the frequency of the mechanical modes of the mirror suspensions. Table 2 lists these frequencies, as given in the PSS list. The identification of the mode is done using the information contained in reference [8] where the mechanical transfer function of the NE suspension was compared to its SIESTA simulation.

The coherence analysis, described in Section 5 below, revealed that these peaks have large coherence with vertical seismic signals (Figure 5), meaning that they are mostly excited by vertical ground motion. What happens is that there is vertical motion of the towers' IP stage, which is not actively damped (as the horizontal one is), which then excites, by mechanical

| Freq (Hz) | SA resonant mode |
|---|---|
| 0.451 | z-Tx mode |
| 0.479 | z mode |
| 0.545 | z mode |
| 0.579 | z mode |
| 0.623 | z mode |
| 0.796 | z mode |
| 0.846 | Ty mode |
| 1.168 | Ty mode (MIRROR+RM vs MARIO) |
| 1.202 | Ty mode (MIRROR+RM vs MARIO) |
| 1.752 | Tx mode (MIRROR opposite to RM) |
| 1.785 | Tx mode (MIRORR opposite to RM) |
| 3.197 | Tx mode (M IRROR+RM vs MARIO) |
| 3.208 | Tx mode (MIRROR+RM vs MARIO) |

Table 2: Lines from the PSS list which correspond to modes of the Super Attenuators. The assignment is done according to the study in reference [8].

coupling, horizontal degrees of freedom at the level of filter 7. This effect will be cured by the implementation of active vertical damping on all towers.

The group of lines between 1109 and 1112 Hz in PSS list (Table A1) are also related to Super Attenuator modes. Figure 6 shows the amazing structure of peaks (obtained using 200s resolution) around the 1111 Hz line. The 1111 Hz line is a calibration line that modulates the laser frequency. One goal of this line is to measure the mode cleaner modulation frequency error. With this line one can measure the common mode noise level in the dark fringe; laser frequency noise is one such noise. If a mirror tilts then the fringe contrast decreases, and consequently the common mode noise coupling increases. This lack of control of the mirrors is a source of many types of noise, including the observed burst of bursts (BOBs) [6, 7].

The fact that this structure is symmetric around the 1111 Hz line suggests that it is due to amplitude modulation of the central 1111 Hz line. We noticed that values of modulation frequencies (i.e. the distance of peaks from the central line) are typical of Super Attenuator modes. Another hint as to the source of the noise is the similar structure of the 1111Hz sidebands and those of the low frequency component of the alignment signals (Ty), which is shown in Figure 7.

In order to test the modulation hypothesis, we took a simple sinusoidal signal at 1111Hz and modulated it with the alignment error (*Sc_*_tyGc*) signals, then we computed the coherence between the obtained signals and the dark fringe signal. Figure 8 shows the result. Some coherence is found with all alignment signals over a 5 Hz band; the largest coherence is with the signal measuring the NE Ty mirror position.

As part of the same "puzzle" we noticed sidebands with a similar structure (and coherence pattern) also around the calibration lines at 353, 355 and 357 Hz, and as well around the narrow and intense line at 3050 Hz, as shown in Figure 9. (These additional sidebands are not in Table A1, but they are in the PSS list which has higher resolution). All these lines have the common feature to be very narrow and stationary.

The full understanding was provided by the output plots produced by the *NonStatMoni* monitor [5]. [2]One such plot is reproduced in Figure 10. It reveals that the dark fringe signal was modulated with residual mirror angular motion at low frequencies over most of its bandwidth. As a consequence the low frequency angular noise couples to every intense spectral line in the dark fringe which is narrow and stationary (such as calibration lines); this increases the spectral noise nearby. The commissioning plan is to increase the low frequency gain of alignment control loops and thus reduce mirrors slow angular oscillation in future runs.

[2]The *NonStatMoni* program monitors the non stationarity of the dark fringe signal and alignment signals in different frequency bands. This is done by first computing band limited RMS of the data at given time steps (10s, 100s, ...), then looking at the spectral composition of the RMS time series and eventually computing coherences between different RMS series.

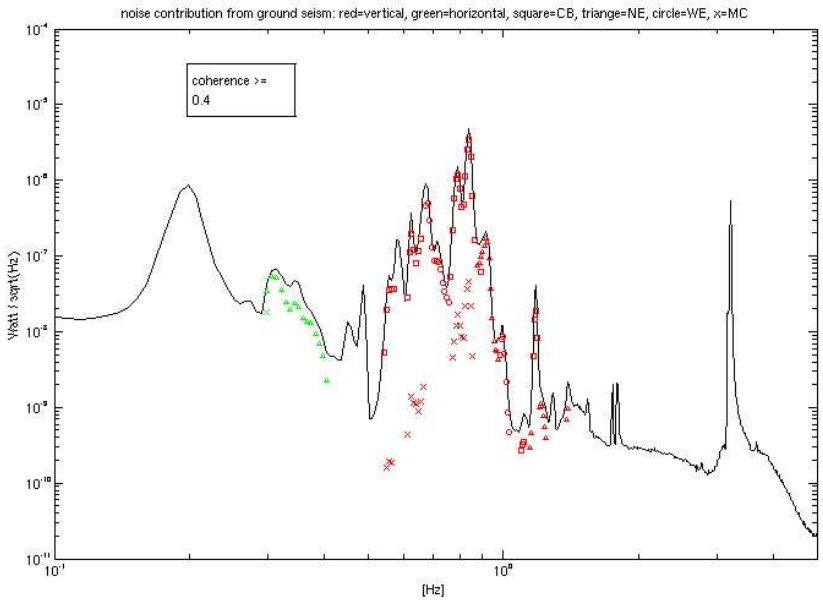


Figure 5: Contributions to the C7 dark fringe photodiode of horizontal (green) and vertical (red) ground seismic motion measured at different buildings: square=central, triangle=NE, circle=WE, cross=MC. Colored points are the projection of the coherence onto the dark fringe spectrum, for frequencies at which coherence is greater than 0.4.

# 5 Lines identification with coherence and multi-coherence tools

A necessary step for the identification of lines originating from electro-mechanical devices in the laboratory is to search for matched coherences between the dark fringe and signals from our environmental monitoring instruments: accelerometers, microphones and magnetometers. Such a search was performed (since C6) by a program tool that computes the coherence in 130s non overlapping sets of data of the dark fringe photodiode *Pr_B1_ACp* (i.e. 7.7mHz resolution) averaged over the entire science mode data segments. The program detects frequency peaks above a cutoff value corresponding to 2.5 standard deviations above the mean coherence in the frequency band of interest, and with a width larger than 0.1 Hz. Plots of coherences and lists ordered by environmental sensor channel or by frequency are posted on the web ($http://wwwcascina.virgo.infn.it/DataAnalysis/Noise/doc/C7/coherence/webpage/catalogue.html$). Figure 11 shows a sample coherence plot. In Table 3 is the list of found matches.

The computation of multi-coherence is necessary in order to measure correctly and disentangle the contribution of one reference signal (i.e. the dark fringe) from the noise measured by several different auxiliary channels (i.e. environmental sensors). This tool is present in the NAP library[9]. It properly accounts for correlations among channels, and gives as output the disentangled noise contributions and the reference signal with the noise removed. We performed a multi-coherence analysis of the magnetic noise in the C7 dark fringe signal (the complete set of plots can be found at *http://wwwcascina.virgo.infn.it/DataAnalysis/Noise/doc/C7/MagneticNoise/*)

Several noise lines and structures have been detected, among which a strong 10 Hz line and its higher order harmonics. The analysis indicates a strong coherence with magnetic channels in the central building, suggesting a source located there. Figure 12 shows the measured contributions from magnetic noise measured by all magnetometer channels. The culprit was then identified as electromagnetic noise emitted from digitization boards for the digital cameras that are located in the data acquisition room (more details in Section 6 below). For a thorough analysis of 10 Hz harmonics and how they affected the PSS analysis of C7 data see document [4]. In Figure 13 we show another interesting result of the multi-coherence analysis applied to magnetic channels; the coherence with magnetic channels is sufficient to completely remove of 50 Hz line from the dark fringe.

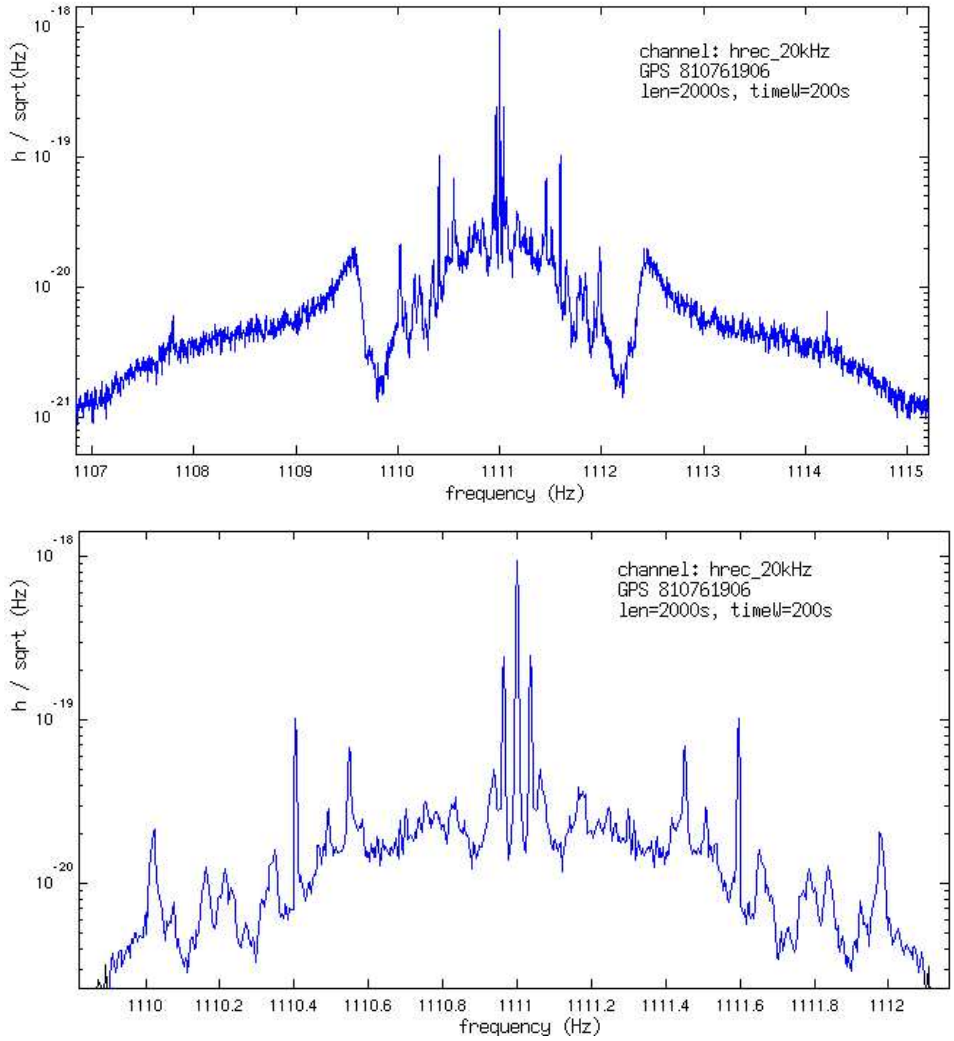


Figure 6: Spectral lines around 1111 Hz. Peaks are located symmetrically with respect to the 1111 Hz. Major ones are at +- 0.0405 Hz, +- 0.449, +- 0.596, +- 0.981, +- 3.21 Hz.

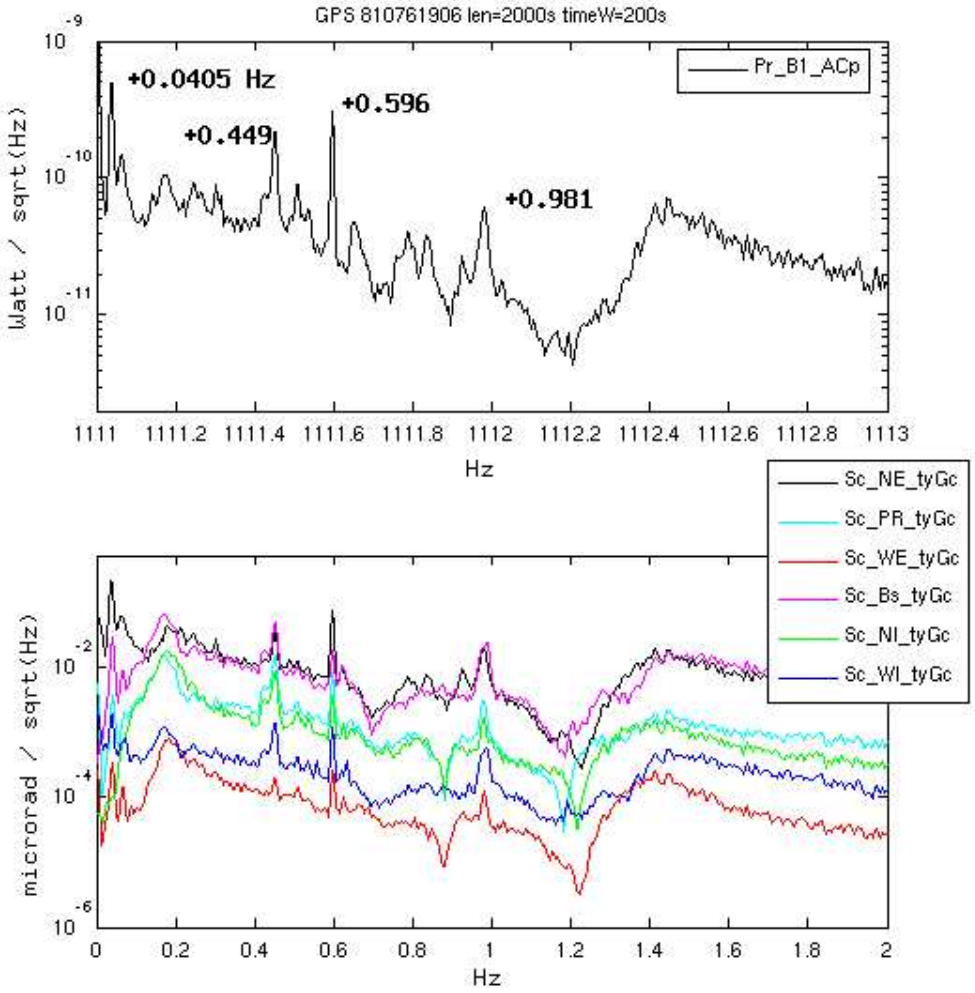


Figure 7: A comparison of one-side of the sidebands of the 1111 Hz line (top) and the low frequency spectral amplitude of alignment error signals (bottom). It is apparent that this low-frequency noise is modulating the 1111 Hz line.

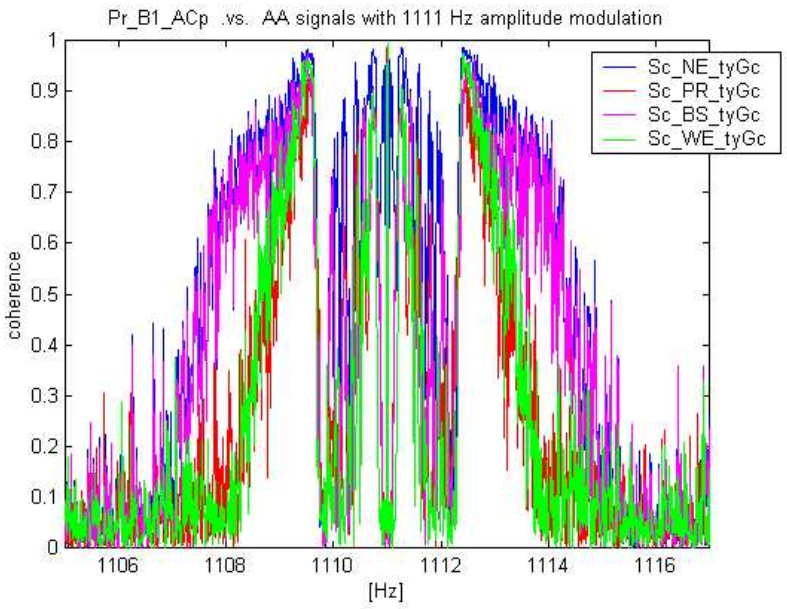


Figure 8: Coherence of the alignment error signals and the dark fringe signals in the vicinity of 1111Hz.

| frequency [Hz] | SNR | width [Hz] | Match in coherence catalogue: close (?) or exact (!) |
|---|---|---|---|
| 20.14 | 486 | 0.01 | (!) seismometers and microphone WE |
| 192.13 | 449 | <0.01 | (!) seismometers and magnetometers CE |
| 42.09 | 399 | 0.02 | (!) magnetometers NE |
| 16.63 | 376 | 0.1 | (?) seismometers and microphone MC at 16.69 Hz |
| 38.4 | 360 | <0.01 | (?) Em_SEDBWE01 at 38.22 Hz, Em_ACBDNE01 at 38.24 Hz, Em_SEDBNE01 at 38.275 Hz |
| 6.88 | 326 | <0.01 | (?) Em_MABDNE02 at 6.614 Hz |
| 14.8 | 187 | 0.01 | (?) Em_ACLALL01 at 14.69 Hz |
| 25.58 | 185 | 0.01 | (!) magnetometers NE |
| 19.29 | 121 | 0.03 | (!) magnetometers NE |
| 19.43 | 67 | 0.01 | (!) magnetometers WE |
| 25.02 | 114 | 0.02 | (?) Em_SEBDMC01 25.174 0.37053 |
| 31.89 | 106 | 0.05 | (!) acoustic and seismic NE |
| 33.75 | 88 | 0.02 | (?) Em_SEDBNE01 at 33.716 Hz and Em_ACBDNE01 at 33.727 Hz |
| 21.26 | 67 | 0.03 | (!) acoustic and seismic NE |
| 31.52 | 63 | 0.01 | (!) acoustic and seismic WE |
| 43.86 | 67 | 0.03 | (?) Em_SETOPR01 at 42.873 Hz |
| 32.89 | 33 | 0.03 | (!) seismometers WE |
| 46.76 | 29 | 0.01 | (!) seismometers and microphones in CE, including laser lab and det.lab. |

Table 3: Matches between the dark fringe lines from PSS and peaks that were found with the environmental coherence catalogue.

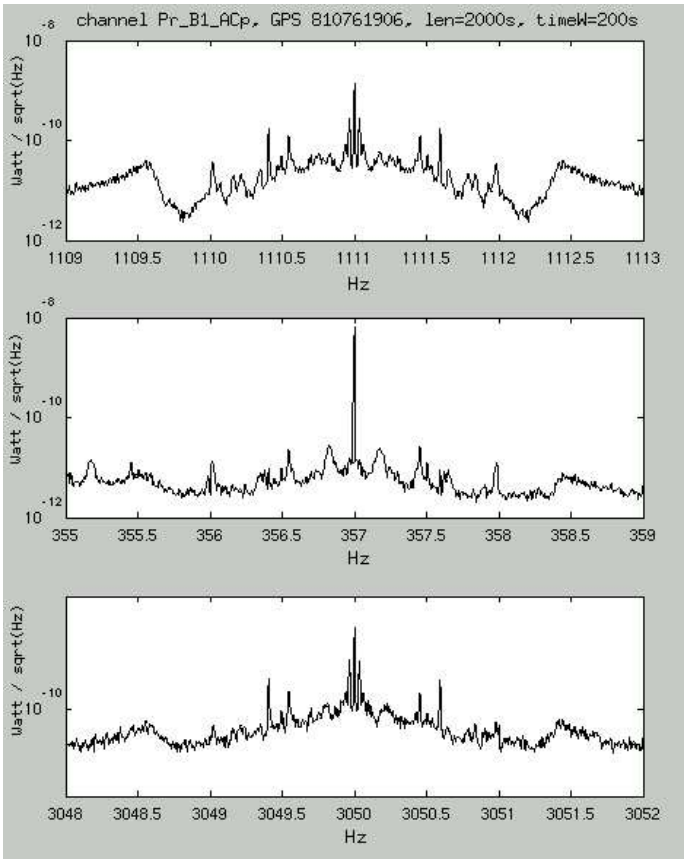


Figure 9: Sidebands in Pr_B1_ACp around intense and narrow lines at 1111 Hz (calibration), 357 Hz (calibration) and 3050 Hz (unknown).

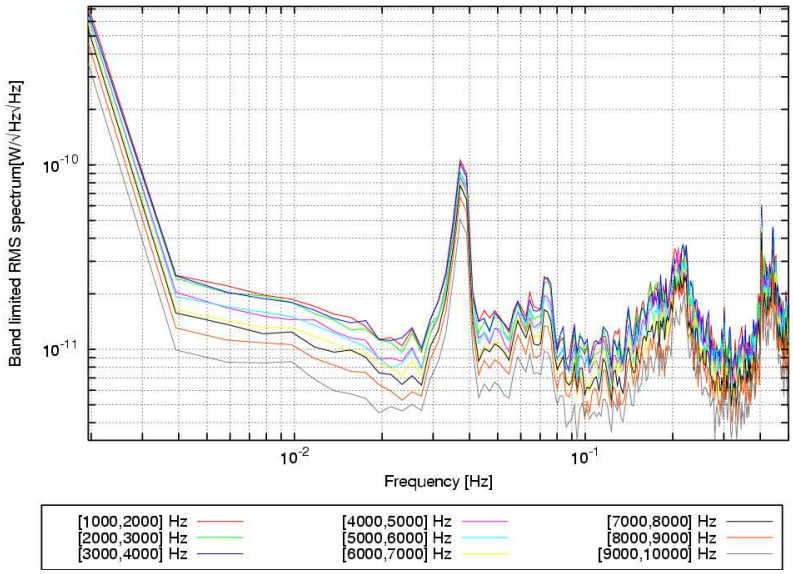


Figure 10: Spectral composition of band limited RMS of Pr-B1-ACp signals (this plot is automatically produced by *NonStatMoni*)

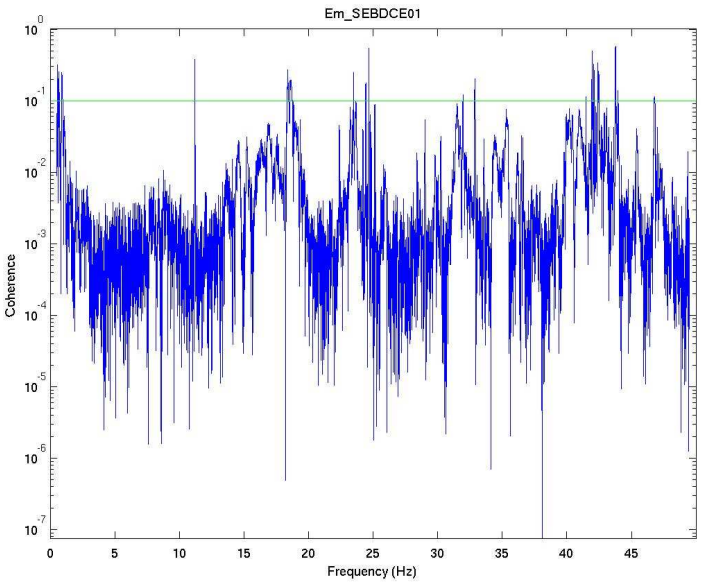


Figure 11: Sample coherence plot from the *Environmental Coherence Catalogue*. This coherence example was calculated between channels Pr_B1_ACp and Em_SEBDCE01.

# 6 Experimental search of line sources

Using as a guideline our list of matches with the environmental coherence catalogue (Table 3) we went hunting in the laboratory for the sources of the line noise. Our portable equipment consisted of: one accelerometer (piezo accelerometer model 393B12 by PCB with 0.1Hz to 4kHz bandwidth, and sensitivity $10^4$mV/g), one microphone (CEL-231 by Casella, 10 Hz to 25 kHz bandwidth, dynamic range 30 to 135 dB, 1dB accuracy), one magnetic probe (tri-axial Hall effect sensor by Honeywell model HMC2003, spectral sensitivity 40 $\mu$Gauss over 1kHz bandwidth, expected noise floor 4nT/$\sqrt{1000}$=0.13nT) and one spectrum analyzer (Onosokki CF 6400) used for data read out. Below we describe the several measurements performed.

## 6.1 Turbo pump cooling fans

Two "horns" at about 45 Hz appeared in the C7 dark fringe data (Figure 14-top), and are particularly intense during the first 25 hours of the run. They have strong a coherence with seismic sensors inside and around the laser laboratory (Figure 14-bottom). On the other hand, the coherence with acoustic sensors is negligible.

During the run on the morning of September 18th 2005, as a test, all turbo pumps were switched off in rapid sequence. The horns promptly and completely disappeared from the dark fringe signal in correspondence with the turn off of the IB tower's turbo pump.

Through our measurements in the laboratory, we discovered that the source of this noise are the two little cooling fans on the turbo pump enclosure. The small difference in rotation speed of the two fans accounts for the two slightly displaced spectral peaks. In Table 5 we provide the measured signature frequencies of the cooling fans for all turbo pumps in the central building. For this measurement we placed the portable seismometer upon the turbo pump vessel. At the same time we measured no magnetic noise, nor any significant acoustic noise produced at these frequencies.

Figure 14 shows another interesting feature; the presence of the horns in the dark fringe signal were reduced in amplitude in correspondence with the (manual) tuning of the laser modulation frequency to match the mode cleaner cavity length. Also shown in Figure 14 is that there is additional dark fringe noise in the 35-50 Hz region around the horns, which have

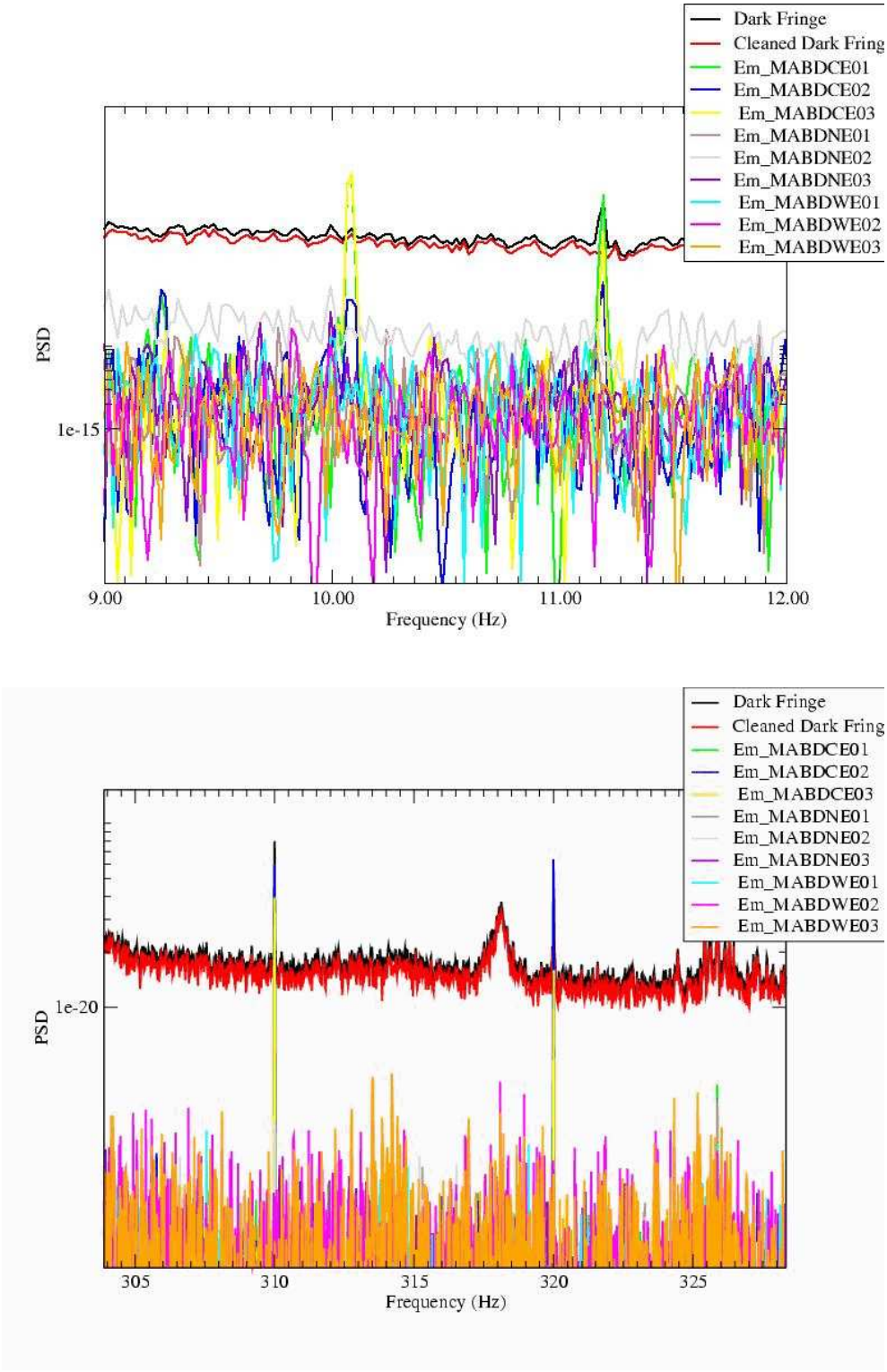


Figure 12: The 10Hz line and its harmonics in the dark fringe and the measured contributions from magnetic noise (2 plots).

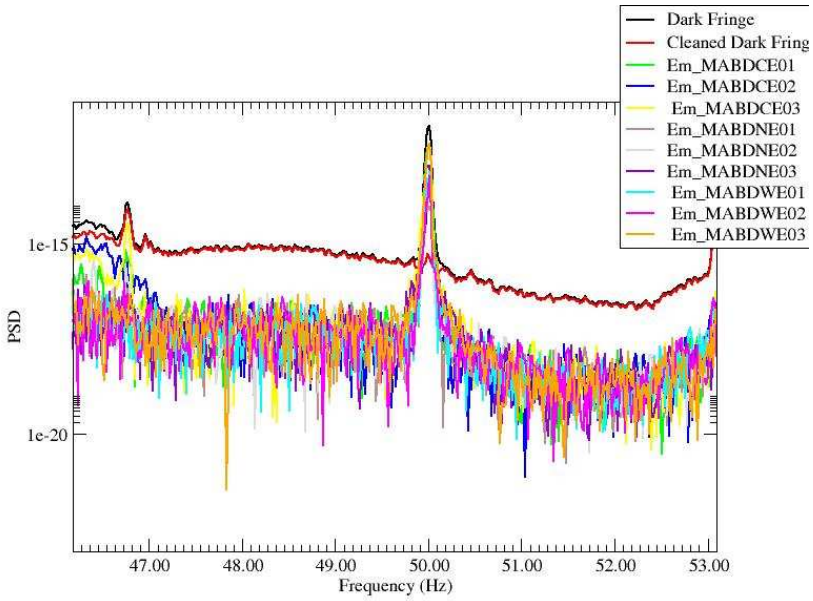


Figure 13: Magnetic noise contributions to the 50 Hz line in the dark fringe signal measured by all our magnetic channels.

| SA tower | Frequency and amplitude of first horn | second horn | rotor speed [Hz] |
|---|---|---|---|
| PR | 45.01 Hz 31.36 mV | 45.37 Hz 45.78 mV | 600.7-600.84 Hz 270-310 mV |
| BS | 45.0 Hz 15.73 mV | 45.57 Hz 26.21 mV | 600.7-600.8 Hz 450-480 mV |
| WI | 45.14 Hz 32.41 Hz | 45.3 Hz 16.46 mV | 600.6-600.81 Hz 170-200 mV |
| DE | 44.7 Hz 1.6 mV | 48.22 Hz 2.5 mV | 600.7-600.8 Hz 390-400 mV |
| SR | 45.19 Hz 28.6 mV | 45.35 Hz 23.03 mV | 601.4-601.5 Hz 0.9-1.0 V |
| IB | 45.22 Hz | 45.42 Hz | 601.5 Hz |
| NI | pump was off at time of measurements | | |

Table 4: Frequency and amplitude of the most intense seismic peaks from turbo pumps in the central building: the two cooling fans, and the pump rotor. Measurements were taken with a portable accelerometer placed upon the turbo pump metallic enclosure.

similar characteristics as the horns; it is coherent with the same seismic channels and it reduces with the tuning of the modulation frequency. Another common feature of this noise and the horns is the strong coherence with the angular noise of the IMC cavity optical axis, mainly along $\theta_y$ d.o.f. We suspect this additional noise to be produced by other mechanical devices inside and around the laser laboratory.

We do not have a clear understanding of the path by which this turbo pump noise enters the dark fringe, but one possibility is the following: as described in Ref. [10], a mismatch between the modulation frequency and IMC length causes IMC longitudinal noise (mainly IB resonances) to couple into the ITF sensitivity through the BS control loop. Seismic noise in the laser laboratory, and vibrations of the external optical bench, produce jitter of the laser beam entering the IMC. This is IMC angular noise that can then convert into longitudinal noise in the presence of an offset of the optical axis.

## 6.2 Hunting the line sources

The list of frequency peaks from the environmental coherence catalogue matching with PSS lines (Table 3) gave us clues as to the location and type of the noise source. Using this information, we performed measurements on the magnetic, seismic, and acoustic noise emissions by the air conditioners and other major noise sources in the DAQ room, and the

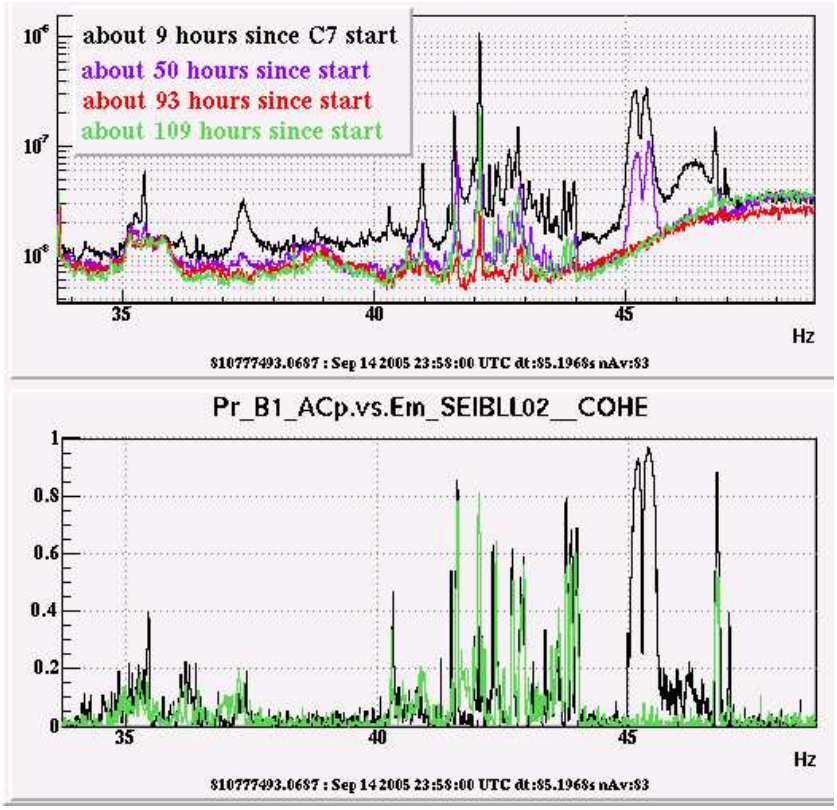


Figure 14: The *horns* at about 45 Hz and nearby noise in C7 dark fringe photodiode at various times during the run: (top) dark fringe photodiode spectrum, (bottom) dark fringe coherence with an accelerometer on the external injection bench. The plots show how the horns disappear when IB turbo pump is switched off after $50^{th}$ hour. The top plot shows that the amplitude of the nearby noise increases with the detuning of the modulation frequency. The noise is coherent with seismic noise in and around the laser laboratory.

| Air Conditioning NE | | |
|---|---|---|
| Frequency[Hz] | microphone[$Pascal/\sqrt{(Hz)}$] | accelerometer on the bench $[m/s^2/\sqrt{(Hz)}]$ |
| 19.2 | 7.3e-003 | 9.7e-005 |
| 20.3 | 1.3e-002 | not seen |
| 31.6 | 3.0e-002 | 6.1e-004 |
| 33.6 | 1.7e-002 | 2.8e-004 |
| 52.7 | 3.0e-002 | 2.2e-004 |
| 57.5 | 1.9e-004 | not seen |
| Air Conditioning WE | | |
| 9.12 | 0.0145 | not seen |
| 19.44 | 0.0086 | 0.00019 |
| 31.70 | not seen | 0.00022 broad peak |
| 33.06 | not seen | 0.00031 broad peak |
| 38.87 | 0.0074 | 0.00014 |
| 54.96 | 0.013 | 0.00095 |
| 58.32 | 0.0069 | 0.00041 |
| 73.28 | 0.010 | not seen |
| 77.7545 | 0.0369 | 0.00078155 |

Table 5: The most intense lines from the NE and WE air conditioning. All lines have spectral width of about 0.1 Hz, and are seen to drift in time by about $\pm$ 0.3 Hz. The time resolutions used for the FFTs used in these measurements were 81 s for the microphone and 13 s for the accelerometer.

North and West experimental halls.

Figures 15 to 17 compare acoustic spectra recorded with air conditioning on and off. Table 5 lists the most intense frequency lines produced by the air conditioning in the WE and NE buildings. Some of these noise lines were found in the C7 dark fringe signal (see Table A1).

We investigated the possible coupling of the air conditioner noise to the terminal optical benches. We probed the air conditioning noise with the accelerometer and microphone deployed in different locations inside the NE hall (using the 31.7 Hz line as reference). We measured the most intense noise (31.7 Hz line amplitude) at the tube linking the bench enclosure to the NE tower. We also found that, while acoustic noise is the same everywhere, seismic noise is stronger on the bench and on top of the bench enclosure than it is on the floor around the bench or at the bench support; see Figure 18). Thus, we suspect that the major coupling of the air conditioning noise to the bench is not seismic (i.e through table legs) but acoustic (i.e. air pressure noise shaking optics on the bench and possibly also the link tube). A possible path to the dark fringe is through diffused light, which is re injected into the interferometer after being scattered by some optical component on the bench, as explained in Ref. [11].

Searching the central building for strong 10 Hz magnetic emissions with our portable magnetic probe we found the source of the 10 Hz harmonics to be the boards in rack number 56 in the DAQ room. These boards receive the analog signal from the cameras and subsequently digitize them. To do so they send a 10 Hz timing signal to digital cameras 15 to 19.

While searching for the 10 Hz noise source we also discovered the source of a 10.1 Hz noise line. Although not affecting ITF sensitivity, this noise line is quite intense in the central building magnetic sensors. This 10.1 Hz noise is generated by the DAQ room air conditioning machine that is located inside the room. It is actually quite surprising how this magnetic line (its magnetic nature is also confirmed by the fact it is narrow and very stationary) can be generated. However, its origin is confirmed by its disappearance in correspondence to air conditioning switch off (Figure 19).

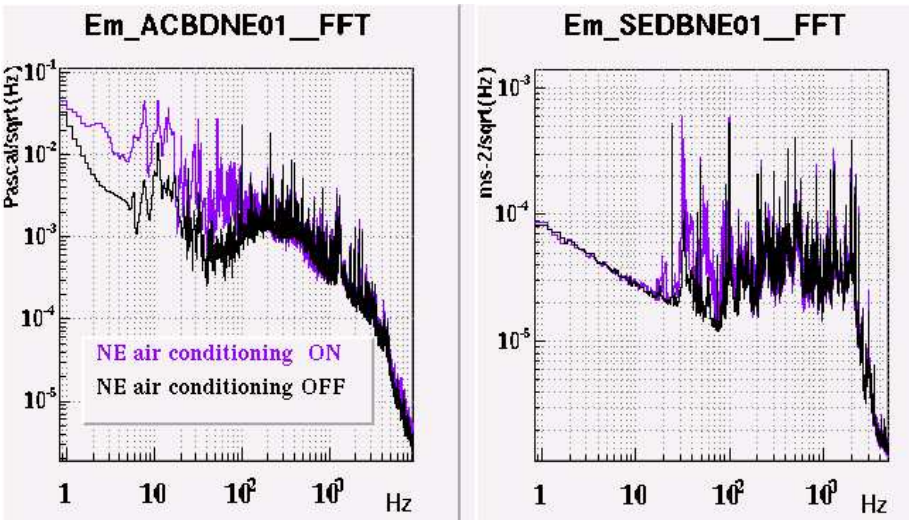


Figure 15: The reduction of acoustic (right) and seismic (left) noise consequent to the switch off of the air conditioning in the NE building.

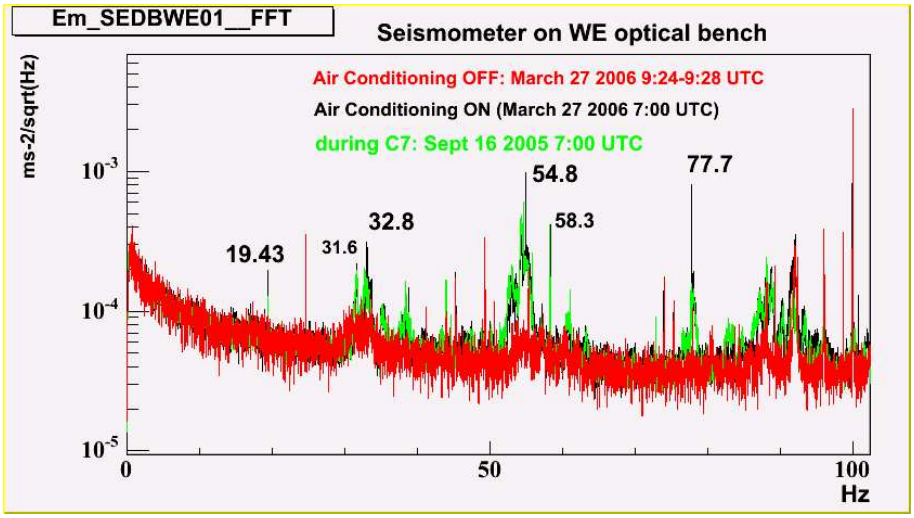


Figure 16: Identification of lines from the WE air conditioning. These were determined by comparing seismic spectra recorded with the air conditioning device off and on.

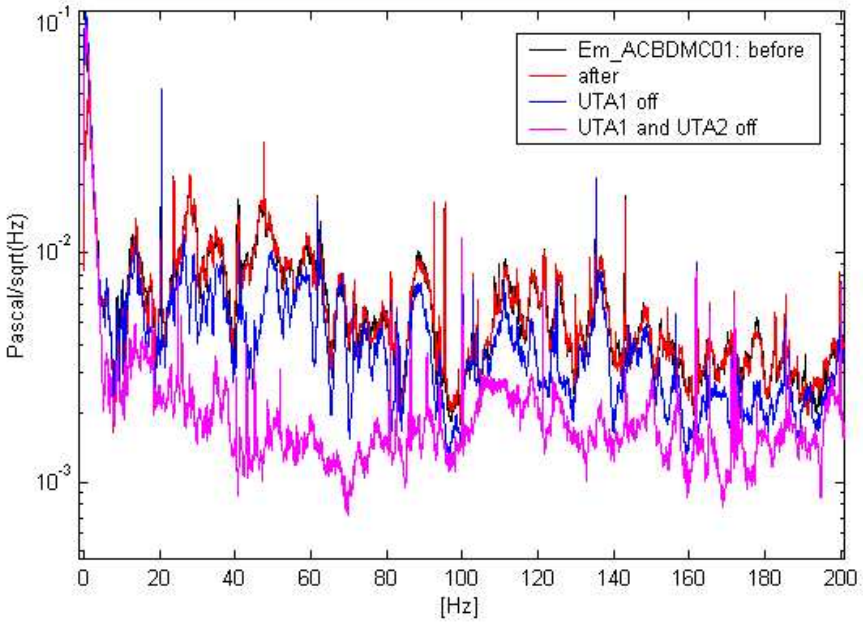


Figure 17: Acoustic noise reduction in the MC building consequent to the turn off of the two air conditioning units, UTA1 and UTA2.

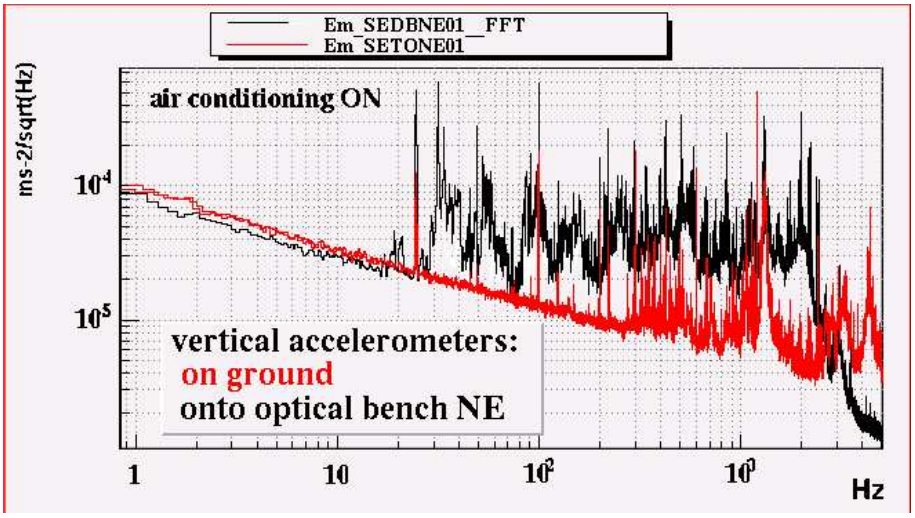


Figure 18: Seismic noise on the ground and on the NE external optical bench.

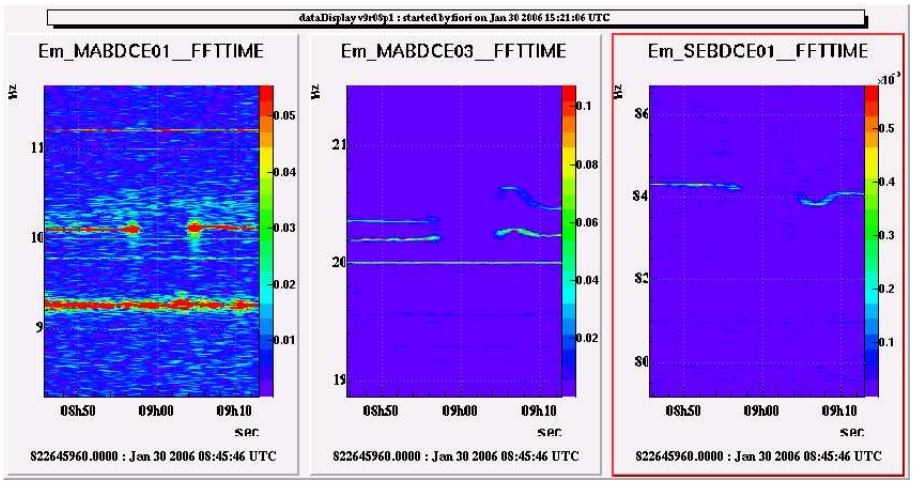


Figure 19: Spectrograms showing the disappearance of a 10.1 Hz line, and its harmonics (left and middle plot), from the magnetometer signal in the central building (located on the balcony above the DAQ room) in correspondence with the turn off of the DAQ room air conditioning unit. The right plot shows an associated spurious line in one of the seismometer channels.

# 7 Mirror and violin modes

At least eight of the resonant modes of the large mirrors have been identified from the lines observed by the PSS: these are the NE, WE, NI and WI butterfly (about 3885 and 3917 Hz) and drum (about 5545 and 5584 Hz) modes (see Figure 20). These values correspond to the theoretical prediction [13]. A variation of few hundreds of Hz of the mode frequency is observed during C7 and can be associated to a change in the mirror temperature due to temperature changes in the tower ovens. The identified line at 7724 Hz resembles a Lorentzian peak (Figure 20). It is candidate for being the internal mode (0,1) ($drum$) of the BS mirror. The theoretical prediction for this mode is 7740 Hz [13].

The group of lines in the range 330–340Hz, are the fundamental violin modes of the four wires suspending the NE, WE, NI, WI mirrors, which are thermally excited (Figure 21). These are, in fact, predicted to be at about 320Hz [12]. In the PSS list, with 1000 s time resolution, we identified 28 distinct peaks. Actually, we expect 32 distinct fundamental modes. This is because wires tension cannot be perfectly equalized, and z-x degeneracy is actually removed since the wires are clamped to finite mass bodies with not-diagonal moment of inertia (i.e. $I_{xz} \neq 0$). Higher modes, up to the $4^{th}$ order, are detected by the line search programs (also shown Figure 21). Figure 22 shows that the higher order modes are not exact multiples of the fundamental ones; this is actually due to the fact that each excited wire is actually a coupled oscillator because it has non-negligible couplings with the marionette and mirror eigenmodes [3].
The BS mirror is about four times lighter then the input and end mirrors (5 kg vs. 20.3 kg)[12][14]. Thus the four violin modes of the BS wires are predicted to be at about 160Hz. They are actually found at about 167Hz. The 167 Hz peak is composed of four close peaks, between 167.2 and 167.6 Hz.

## 7.1 Ring down of violin and mirror modes

Mirrors and wires are mechanically excited at each lock acquisition and decay to a stationary state within 500-1000s after the lock is acquired. The transient period is observed by looking at the spectrogram of the whitened dark fringe signal (Figure 23).

A measurement of the decay time of these modes (i.e. a measurement of $Q$) is interesting because it provides information on the characteristics of the mirrors; the $Q$ is linked to the loss angle for the dissipation mechanism. The expected $Q$ value

[3]The legrangian function for a system of $n$ coupled oscillator has a general form: $L = \sum a_{i,j}\dot{x}_i\dot{x}_j + b_{i,j}x_ix_j$. To compute the normal modes of $n$ coupled oscillators one has to solve the system of $n$ lagrangian equations. Solutions are non linear functions of the proper modes: $\Omega_j = F_j(\omega_1, \omega_2, ..., \omega_n)$ Thus, the higher mode of order $m^{th}$ is: $\Omega_{j,m} = F_j(m\omega_1, m\omega_2, ..., m\omega_n)$, which does not scale linearly with $m$.

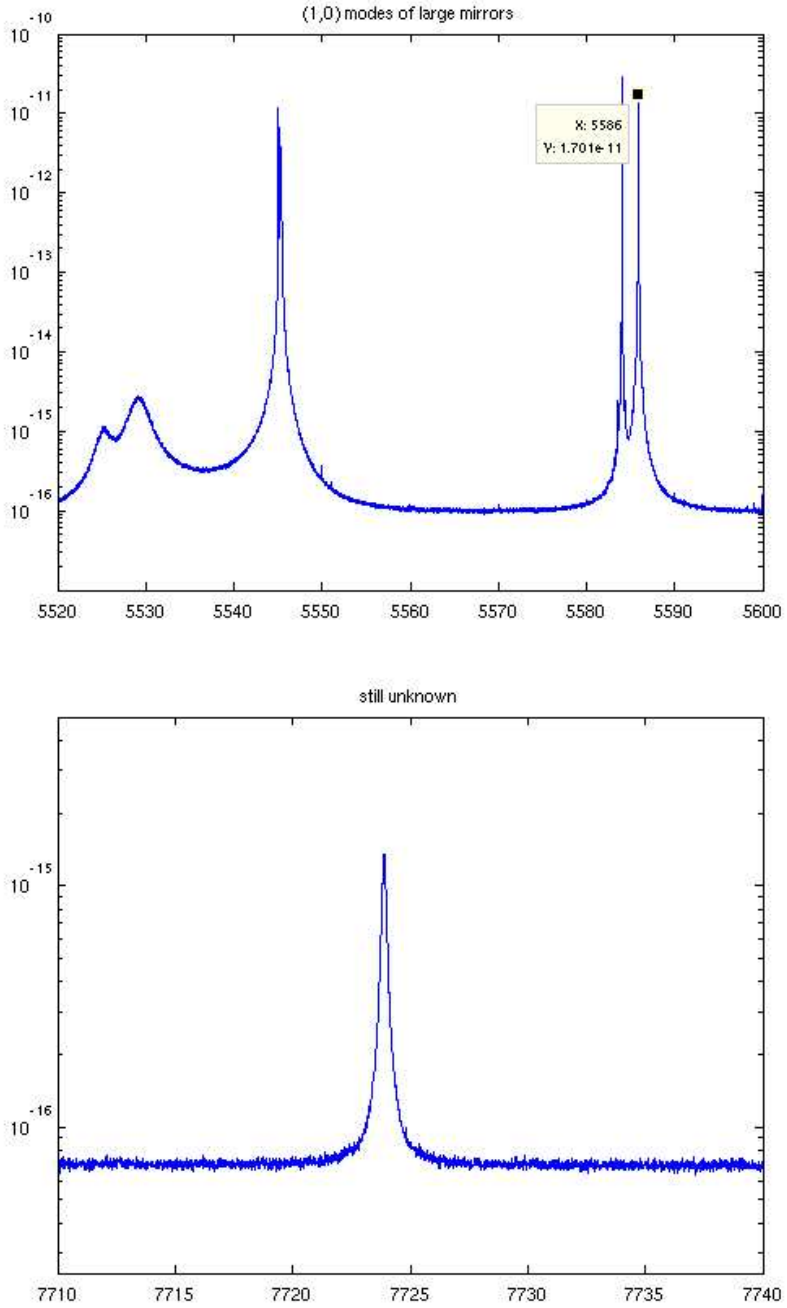


Figure 20: Identified mirror *drum* modes (top) and the candidate drum mode of the BS mirror (bottom) in the C7 dark fringe photodiode signal.

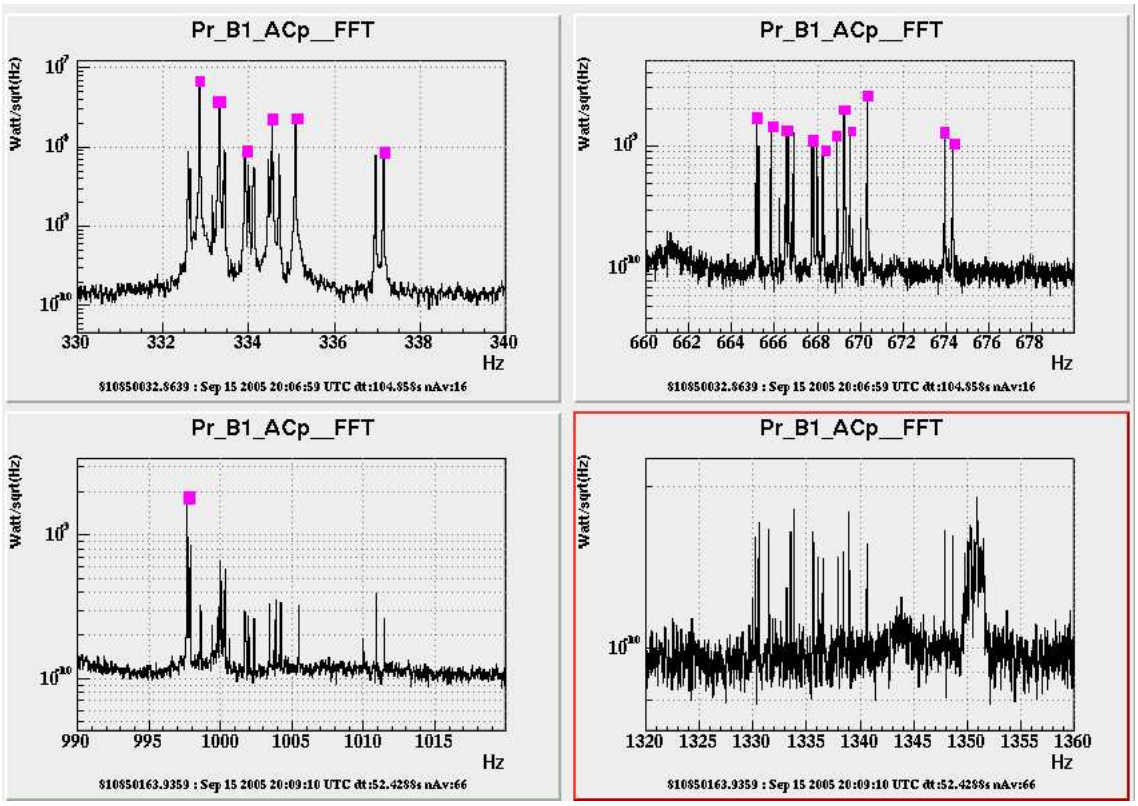


Figure 21: The $1^{st}$ to $4^{th}$ order violin modes of the mirror suspension wires as seen on the Pr_B1_ACp photodiode spectra (with 100 s resolution). Square points mark the peaks identified by the line search algorithm run (with 13s resolution).

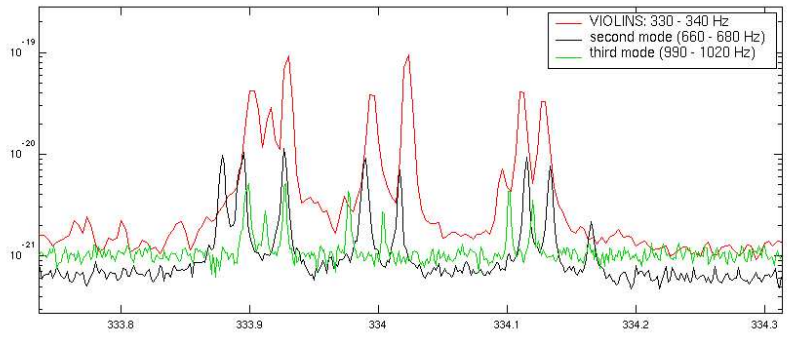


Figure 22: Zoom in of the overlap of some fundamental violin modes and their second and third harmonics.

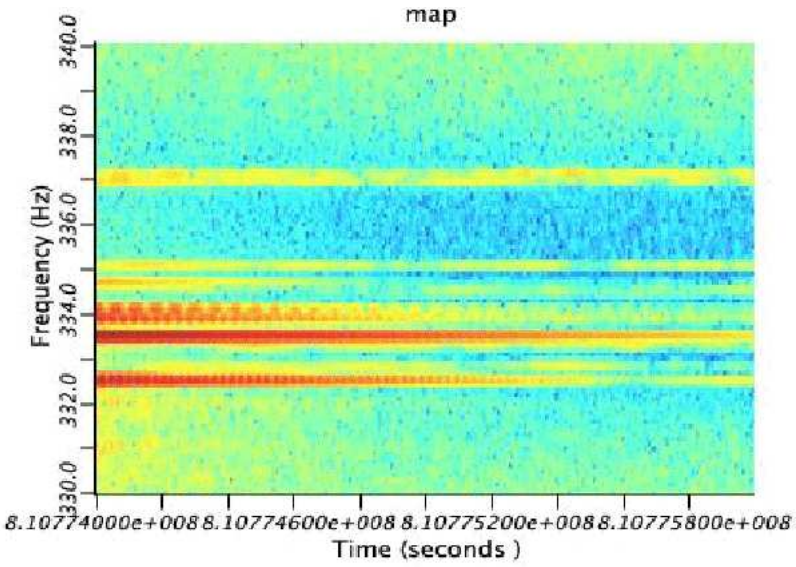


Figure 23: Time frequency map of 1800 s of whitened dark fringe data, starting right after a lock acquisition. This shows the ring down of some violin fundamental modes. The most highly excited ones likely correspond to the NI mirror which receive the correction signal for the lock acquisition.

| Freq(Hz) | description of mode | expected Tau (s) | Tau (s) |
|---|---|---|---|
| 3884 | NE and WE mirrors: "butterfly" mode | 111 | $106 \pm 7$ |
| 3916 | NI and WI mirrors, butterfly mode | 130 | $510 \pm 40$ |
| 100-200 | BS wires, violins (largest peak at 167 Hz) | | $552 \pm 23$ |
| 300-400 | NE,WE,NI,WI violins | | $520 \pm 27$ |
| 600-700 | NE,WE,NI,WI violins ($2^{nd}$ mode) | | $214 \pm 13$ |

Table 6: Decay times of mirror and wire modes as measured by an exponential fit to the band limited RMS noise and lines' amplitude computed by the *NonStatMoni*. The "expected Tau" column lists the decay times of mirror modes measured in C2 [12] by purposely exciting the individual mirrors.

for the 3900 Hz mirror drum mode ranges from $4 \times 10^5$ to $1.2 \times 10^6$ which corresponds to decay times from 34 to 98 s ($Q = \pi f \tau$)[12][16].

A rough measurement has been performed using the band limited RMS and lines' amplitude data computed by the *NonStatMoni*. The decay times listed in Table 6 are computed by fitting the data with an exponential decay ($Ae^{-t/\tau}$) (see the example in Figure 24). The estimate has been repeated for several (N= 13 to 20) lock acquisitions and the average values are listed in Table 6. Errors are computed as $\sigma/\sqrt{N}$, where $\sigma$ is the standard deviation of the sample of repeated measurements.

These are rough estimates since the RMS computation adds to the real frequency peak a significant amount of noise. An effective measurement could be done by extracting the single monochromatic signal with adaptive filters and perform a fit of its decay amplitude.

We tested this procedure on the butterfly modes of the end mirrors. We used about 200s of the dark fringe photodiode signal ($Pr\_B1\_ACp$ sampled at 20kHz) starting at GPS time 81774196, that is right after a lock acquisition is concluded (i.e. ALP "step 12" is set). We first filtered these data with an adaptive notch filter with center a frequency equal 3884.17 Hz, which corresponds to the frequency of the NE mirror mode. In order to reduce the number of fit points we first shifted the frequency of the mode by modulating the signal with a sinus wave at 3380 Hz and then downsampled the to 10 Hz. In this was the number of points was reduced from about 40 millions to about 2000 which could be managed by the fit

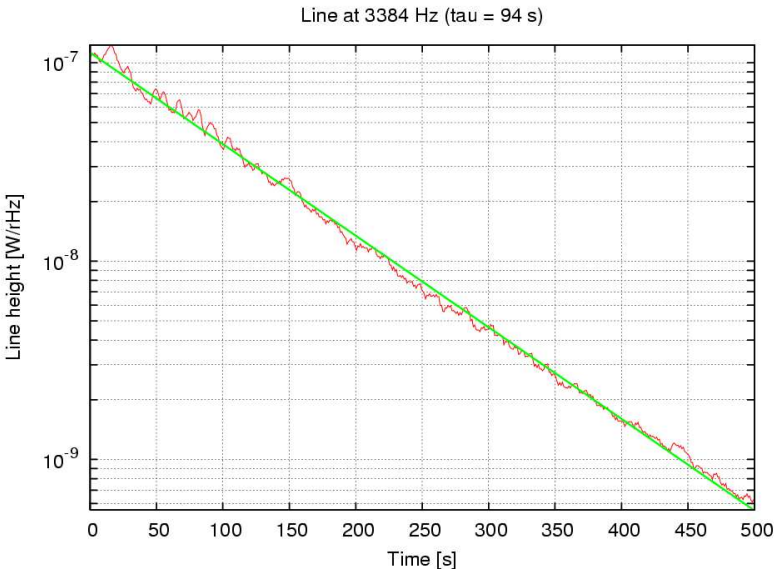


Figure 24: Decay of the amplitude of the frequency line(s) at $3884 \pm 1 Hz$ after one lock acquisition. The green line is an exponential fit with a ring-down lifetime of 94 s.

program. The peak frequency of the NE mirror mode was thus shifted from 3384.17 Hz to 4.17 Hz, but we did not loose any information useful for the fit. The spectra of the downsampled signal is in Figure 25(top). We then fit the signal to the function:

$y(t) = a_1 * \exp -t/\tau_1 * sin(2\pi f_1 t + \phi_1) + a_2 * \exp -t/\tau_2 * sin(2\pi f_2 t + \phi_2)$,

where $f_1 = 4.17 Hz$ (fixed parameter), and the second term accounts for the residual beating with the same mode of the WE mirror which is very close in frequency ($f_2 = 4.60 Hz$, this was set as well as fixed parameter of the fit). We used che CERN package MINUIT, from the PAW program, to perform the fit. We obtain the following result:

$A_1 = 0.862 \pm 0.003$,

$A_2 = 0.820 \pm 0.004$,

$\tau_1 = (118.1 \pm 0.6) s$,

$\tau_2 = (61.3 \pm 0.4) s$,

$\phi_1 = 3.697 \pm 0.002$,

$\phi_2 = 3.003 \pm 0.003$.

The chi squared of the fit is 1.3. Figure 25 shows the result of the fit.

The frequencies of these wire and mirror modes are in the audible band (about 20 Hz to 20 kHz), and the first violin modes are close to a *"MI"* tone (329.63 Hz). We have isolated some of these wires and mirror sounds by applying a narrow band pass filter. Audible (*.wav*) files are stored at *http://wwwcascina.virgo.infn.it/DataAnalysis/Noise/doc/musicaRing-Down/*. These files have been used, together with other "Virgo sounds", in a musical performance, namely part of the celebrations of the 500 years since Galileo Galilei (Pisa, June 2006: *http://www.sidereusnuncius.net/sidereus/index.html*).

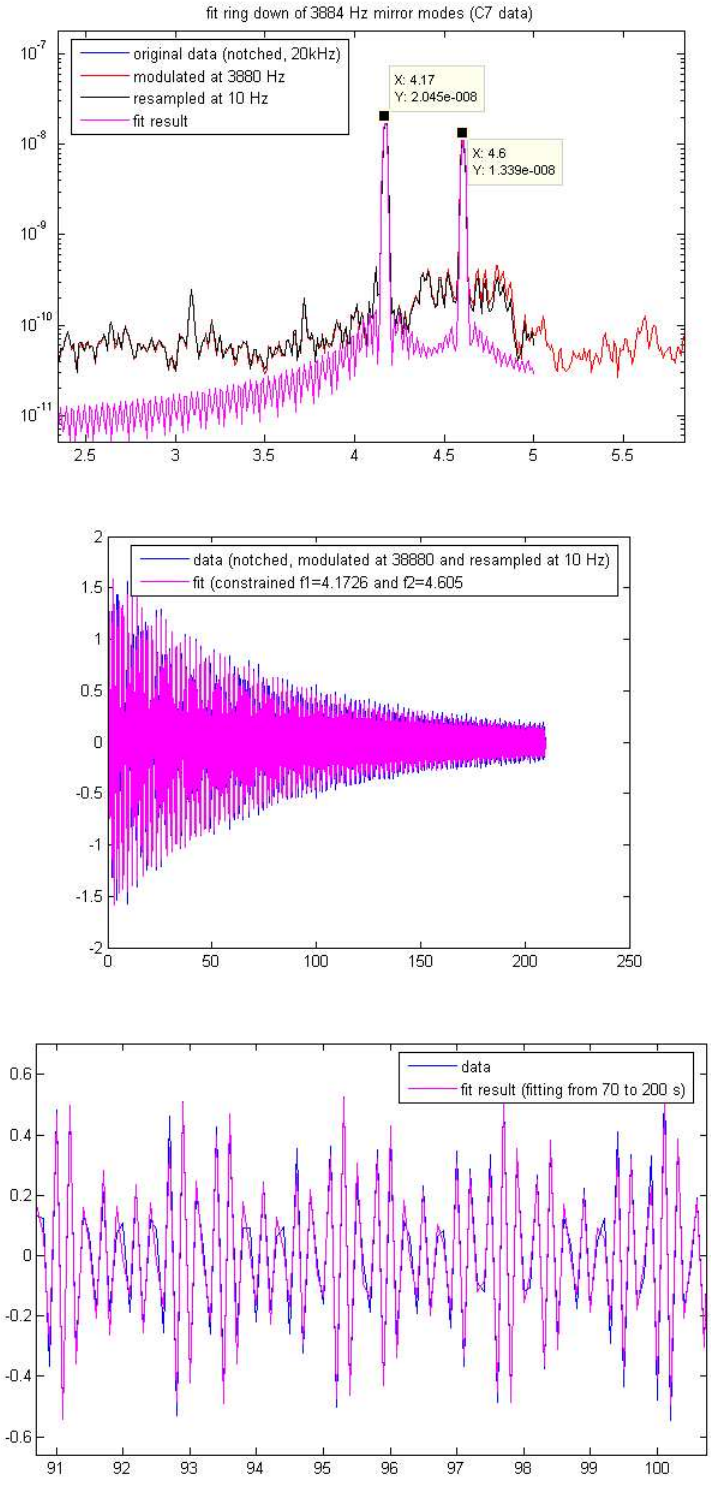


Figure 25: Fit of the 3884 Hz resonances decay. Top plot: spectrum of the signal after the preprocessing steps (notched at 3884 Hz with the adaptive filter, modulated at 3380Hz, and downampled at 10 Hz). The two peaks are the WE and NE mirrors butterfly modes. In magenta is the spectrum of the signal $y(t)$ which is assigned the parameter values resulting from the fit. Units are $Hz$ (horizontal) and arbitrary (vertical). Middle plot: result of the fit over the full time period. Units are $s$ (horizontal) and arbitrary (vertical). Bottom plot: zoom over 10s.

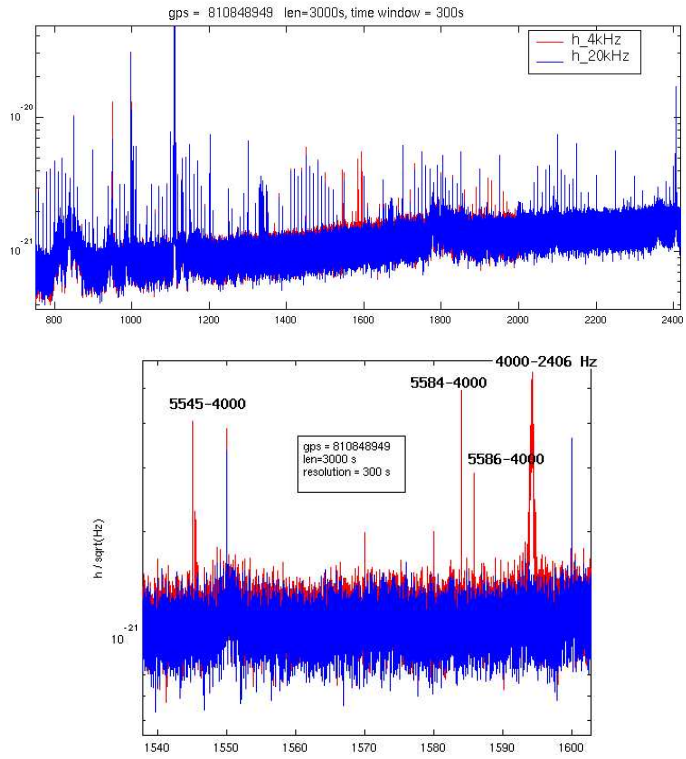


Figure 26: Top plot: aliasing effects in the down sampled h_4kHz data, are evidenced by comparing to h_20kHz data. Bottom plot: few examples of single reflection (2406 Hz line, $4^{th}$ harmonics of turbo pumps) and double reflections (5545, 5584 and 5586 mirror modes).

# 8 Aliased lines

We realized that a few of the lines in the PSS list are the result of the aliasing of higher frequency lines. Figure 26 illustrates one such example. The PSS group used for their analysis the $h\_4kHz$ channel which is the h-reconstructed channel down-sampled from 20kHz to 4 kHz. The down-sampling procedure applies anti-aliasing filtering to the data using one $6^{th}$ order Butterworth with a cut-off at 2000 Hz. Figures 26 illustrates how 300 s spectra are clearly affected by aliasing. Sergio Frasca reported on aliasing effects in PSS searches, and made a proposal for more efficient filters [14].

# 9 Conclusions

We have described the analysis of spectral lines in the dark fringe photodiode signal of C7 run. We adopted, as a new line catalog, the frequency peak list produced by the analysis pipeline of the periodic signal search. This catalog compares well with the output of our line search algorithm. The new method has various advantageous. It profits from the data cleaning performed by the PSS, it has high resolution (at last 1000s, up to 16000s for the low frequencies), and last but not least, being that it is a byproduct of the pulsar search analysis it would come with no additional computational costs. Instead, the search algorithm is to be preferred for the purpose of the on-line monitor of lines that do not require high resolution but quick data access. It could be advantageous to adopt the line selection algorithm implemented within the *NonStatMoni* which currently outputs its list of lines to the frame trend data.

The newly implemented environmental coherence catalog and the multi-coherence applied to environmental channels proved to be very useful tools in identifying lines of environmental origin, and also providing an aid in the location of

these noise sources. Eventually, experimental hunts allowed us to precisely locate the source of several lines. Thus, we were able to identify most of the lines in our list of detected lines. We have stored the information about all detected lines (Table A1) in the on-line line database [15] which has recently been updated and moved to $https://pub3.ego-gw.it/-linesdb/$.

# References


[1] E.Chassande-Mottin I.Fiori, GWDAW 2004, *A simple line detection algorithm applied to Virgo data,* CQG Vol 22, S1189.

[2] S.Frasca P.Astone C.Palomba, *PSS software for the periodic source search* (*http://grwavsf.roma1.infn.it/pss/*) and their presentation to Virgo week february 2006 (*The short FFT database and the peak map for the hierachical search of periodic sources, with the Virgo detector*).

[3] The environmental coherence catalogue: http://wwwcascina.virgo.infn.it/DataAnalysis/Noise/doc/C7/coherence/-webpage/catalogue.html

[4] S.Frasca, Virgo week February 2006. and http://grwavsf.roma1.infn.it/pss/reports/10Hzdeltas.pdf

[5] http://wwwcascina.virgo.infn.it/MonitoringWeb/NonStatMoni/

[6] R. Flaminio, R. Gouaty, E. Tournefier, *Analysis f the sensitivity of the recycled interferometer during C5, C6 and C7 runs*, VIR-NOT-LAP-139-313.

[7] M.A. Bizouard, F. Cavalier , N.Christensen, P.Hello, N.Leroy, *Data Quality and Veto studies for the GW bursts search in C7 run data,* VIRGO-NOT-LAL-337.

[8] I.Fiori S.Braccini F.Travasso A.Vicere', *Siesta simulation of NE suspension tower,* VIR-NOT-PIS-285.

[9] E.Cuoco, GWDAW 2004, *NAP a tool for noise data analysis,* .CQG Vol 22, S1041.

[10] L. Di Fiore, *Modulation frequency/IMC lenght mismatch. Present status and future work,* Virgo Week Feb. 2006.

[11] S.Braccini, *Effect of spurious light coming from end bench*, Virgo Week Feb. 2006.

[12] M.Punturo, VIR-NOT-PER-1390-51.

[13] P.Puppo, VIR-NOT-ROM-1390-262.

[14] P.Puppo, VIR-NOT-ROM-1390-179.

[14] S.Frasca, *About the 4kHz h-reconstructed aliasing problem*, Virgo Week April 2006.

[15] I.Fiori F.Paoletti A.Pasqualetti D.Soldani, *Noise and spectral lines from motor devices,* VIR-NOT-PIS-253.

[16] M.Punturo, F. Travasso, VIR-NOT-PER-1390-263.


# Appendix

In table below we list the lines detected in the dark fringe photodiode signal in run C7 which had SNR above 5. We used the search algorithm and applied the post-processing requests described in Section 2. Frequency resolution of the search algorithm was 13s (0.00763 Hz), and the SRN cut was set at 5. Here we list separately (bottom) the identified 50Hz harmonics. We also indicate the origin of the identified lines. Widths are computed as the number of frequency bins that are merged by the post processing, thus are integer multiples of the frequency resolution.

| Lines detected in C7, channel $Pr\_B1\_ACp$ SNR>5, frequency resolution 0.076Hz | | | |
|---|---|---|---|
| $F_{peak}$ (Hz) | width (Hz) | also in C6 | Comment |
| 0.19 | 0.15 | | |
| 0.69 | 0.31 | | |
| 1.22 | 0.076 | | mirror suspension Ty |
| 3.20 | 0.076 | | mirror suspension Tx |
| 24.64 | 0.076 | | scroll pump IB, reduces after h 25 (tune of mod. frequency) |
| 25.06 | 0.15 | | reduces after h 25 (tune of mod. frequency) |
| 27.85 | 0.076 | | |
| 28.76 | 0.076 | | |
| 31.55 | 0.15 | YES | WE air conditioning, reduces after h 25 (tune of m.f) |
| 41.62 | 0.15 | YES | reduces after h 25 (tune of m.f) |
| 42.11 | 0.076 | YES | NE environment, reduces after h 25 (tune of m.f) |
| 42.88 | 0.076 | | CE environment, reduces after h 25 (tune of m.f) |
| 45.35 | 0.38 | YES | Two horns: 45.22 and 45.42 Hz of IB turbo cooling fans, reduces after h 25 (tune of m.f.) |
| 53.14 | 0.15 | | NE air conditioning, reduces after h 46 |
| 59.74 | 0.076 | | WE air conditioning, reduces after h 25 (tune of m.f.) |
| 103.00 | 0.076 | | calibration line |
| 105.02 | 0.15 | YES | calibration line |
| 107.00 | 0.15 | YES | calibration line |
| 149.57 | 0.15 | | |
| 167.24 | 0.23 | YES | BS wires, 1st violin mode |
| 332.79 | 0.38 | YES | Large mirrors wires, 1st violin |
| 333.37 | 0.15 | YES | Large mirrors wires, 1st violin |
| 334.01 | 0.076 | YES | Large mirrors wires, 1st violin (possibly 2nd violin BS) |
| 335.08 | 0.076 | YES | Large mirrors wires, 1st violin |
| 337.07 | 0.23 | YES | Large mirrors wires, 1st violin |
| 353.01 | 0.076 | YES | calibration line |
| 355.00 | 0.076 | YES | calibration line |
| 357.02 | 0.15 | YES | calibration line |
| 601.46 | 0.15 | YES | Turbo pump IB (rotation frequency) |
| 665.13 | 0.23 | | 2nd violin mode |
| 665.82 | 0.076 | | 2nd violin mode |
| 666.78 | 0.38 | | 2nd violin mode |
| 667.84 | 0.15 | | 2nd violin |
| 668.26 | 0.076 | | 2nd violin mode |
| 668.95 | 0.076 | | 2nd violin mode |
| 669.29 | 0.15 | | 2nd violin mode |
| 669.56 | 0.076 | | 2nd violin mode |
| 670.36 | 0.15 | | 2nd violin mode |
| 673.90 | 0.076 | | 2nd violin mode |
| 674.29 | 0.076 | | 2nd violin mode |
| 997.57 | 0.23 | | 3rd violin mode |

| Lines detected in C7, channel $Pr\_B1\_ACp$ SNR>5, frequency resolution 0.076Hz | | | |
|---|---|---|---|
| $F_{peak}$ (Hz) | width (Hz) | also in C6 | Comment |
| 1109.47 | 0.23 | | 1111 coupling with SA mode (Alignment fluctuation) |
| 1110.04 | 0.15 | | 1111 coupling with SA mode 0.98 Hz (Alignment fluctuation) |
| 1111.00 | 0.076 | | SFSS calibration line |
| 1111.03 | 0.15 | | 1111 coupling with SA mode 0.03 Hz (Alignment fluctuation) |
| 1111.98 | 0.076 | | 1111 coupling with SA mode 0.98 Hz (Alignment fluctuation) |
| 1112.56 | 0.31 | | 1111 coupling with SA mode (Alignment fluctuation) |
| 1202.89 | 0.15 | | IB turbo pump (1st harmonic) |
| 2405.74 | 0.31 | | IB turbo pump (2nd harmonic) |
| 3884.58 | 0.076 | YES | NE and WE mirrors (two close peaks): “butterfly” mode |
| 3916.63 | 0.076 | YES | WI mirror mode, “butterfly” mode |
| 3917.65 | 0.15 | YES | NI mirror mode, “butterfly” mode |
| 4168.89 | 0.15 | YES | |
| 4218.94 | 0.15 | | this is 4168.89 that jumps to 4218.94 at about h 25 |
| 5529.29 | 1.07 | | jumps from 5523.00 at hour 30 |
| 5545.27 | 0.38 | YES | NE and WE mirrors (two close peaks): “drum” mode |
| 5584.07 | 0.15 | YES | WI mirror “drum” mode |
| 5585.90 | 0.15 | YES | NI mirror “drum” mode |
| 7723.92 | 0.076 | | possible: BS mirror mode (0,1) |
| 8605.39 | 0.31 | YES | |
| 9628.87 | 0.15 | | |
| 9629.56 | 0.15 | | |
| 9846.73 | 0.076 | YES | |
| 9849.51 | 0.15 | YES | |
| 9871.90 | 0.23 | | |
| 9872.63 | 0.15 | | |
| 9889.76 | 0.076 | | |

| Lines detected in C7, channel $Pr\_B1\_ACp$ SNR>5, frequency resolution 0.076Hz | | | |
|---|---|---|---|
| Mains and harmonics: 19 lines | | | |
| $F_{peak}$ (Hz) | width (Hz) | also in C6 | Comment |
| 50.05 | 0.19 | YES (49.97 Hz) | |
| 100.02 | 0.23 | YES | |
| 149.99 | 0.34 | YES | |
| 199.97 | 0.31 | YES | |
| 250.02 | 0.42 | YES | |
| 299.99 | 0.11 | YES | |
| 349.96 | 0.49 | YES (350.04 Hz) | |
| 400.01 | 0.69 | YES | |
| 449.95 | 0.076 | YES (449.98 Hz) | |
| 549.93 | 0.77 | YES (550.00 Hz) | |
| 650.02 | 0.99 | YES | |
| 749.97 | 0.42 | YES | |
| 850.07 | 0.46 | | |
| 949.94 | 0.54 | | |
| 999.98 | 0.2713 | YES | |
| 3000.03 | 0.12 | | |
| 3050.00 | 0.52 | YES | |
| 9999.20 | 0.77 | YES | |